Interpreting the $^{13}C/^{12}C$ ratio of carbon dioxide in an urban airshed after correction for humidity interferences

Reporter: Jiaping Xu

2015-5-29

Outline

- 1. Background
- 2. Objective
- 3. Material and Method
- 4. Preliminary results
- 5. Conclusions
- 6. Next Work

1. Background

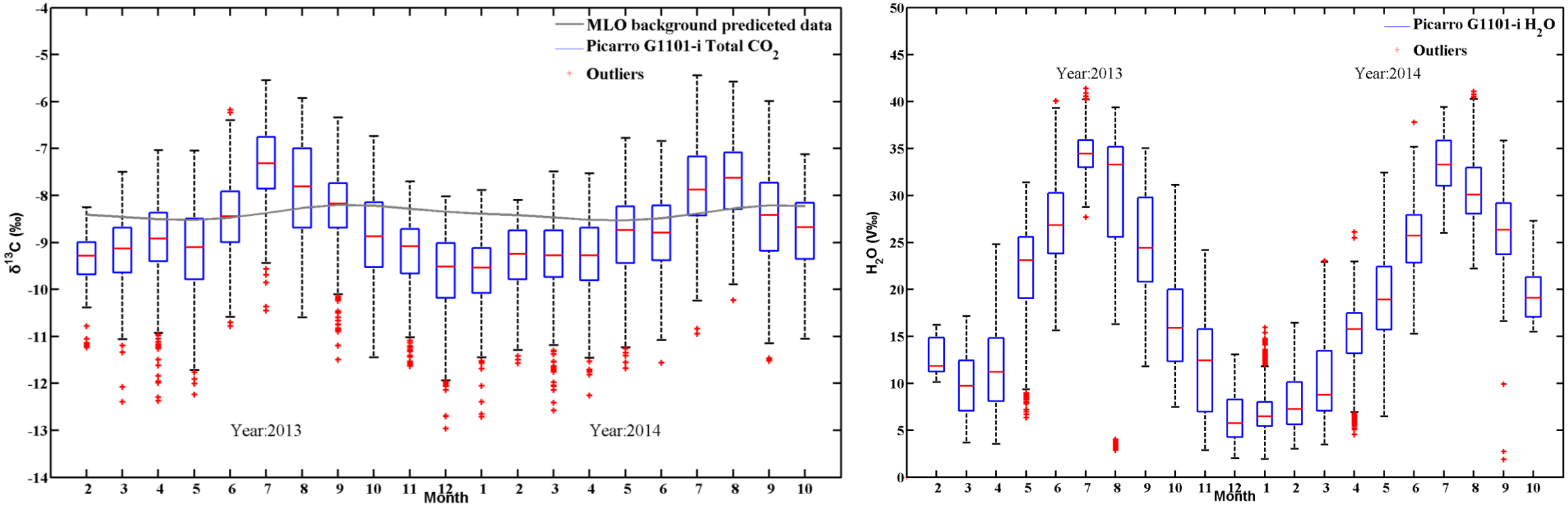

Fig.1 The boxplot of monthly $\delta^{13}C$ and H_2O (**whole data**).

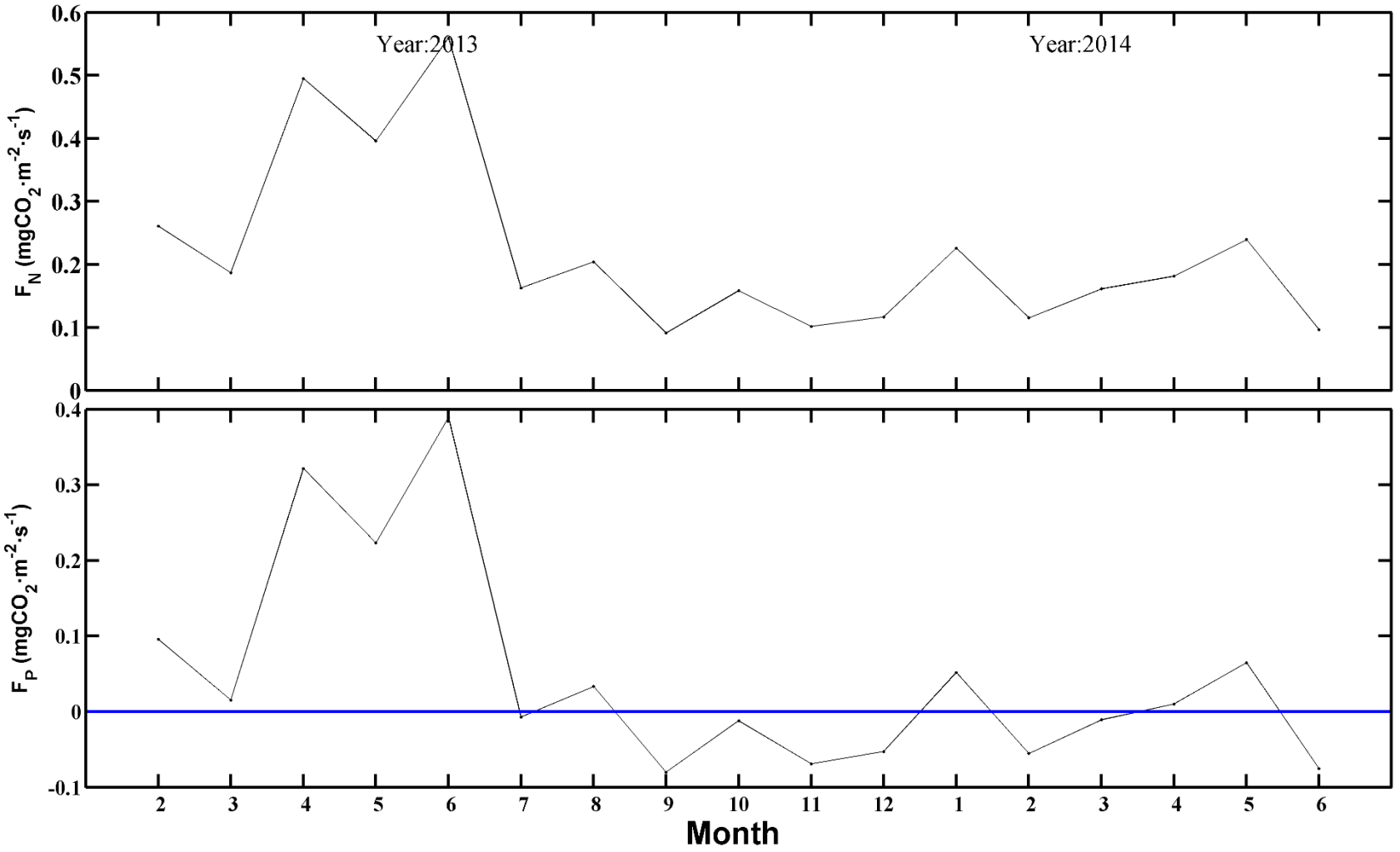

Fig.2 The time series of net CO_2 flux and plant CO_2 flux without humidity correction.

2. Objective

- 1. To correct $\delta^{13}C$ for humidity interferences.
- 2. To calculate monthly F_F, F_P and F_N.
- 3. To partition CO_2 emission contributed by coal and gasoline during winter.
- 4. To investigate the relationship between CO_2 emission and other air pollutants(SO_2, NO_X and CO).

3. Material and Method

Table 1. Dataset of Picarro.

Sites	Period of time
Nanjing	Mar, 2013~ Feb, 2015

Table 2. Cycling of measurement.

Gases	Lasting Time (min)
Standard gas 1	5
Standard gas 2	5
Ambient air	170

Table 3. Information of standard gases.

Standard Gases	CO_2 concentration (ppm)	$\delta^{13}C$ *(‰)	Working period
1 Low	380	-29.75±0.27	Mar, 2013 ~ Aug, 2014
1 High	500	-20.01±0.18	Mar, 2013 ~ Aug, 2014
2 Low	381	-29.75±0.27	Sep, 2014 ~ Feb, 2015
2 High	499	-20.01±0.18	Sep, 2014 ~ Feb, 2015

* (n=41) Results from CAAS and CAFS.

The performance of $\delta^{13}C$ on high H_2O mixing ratio

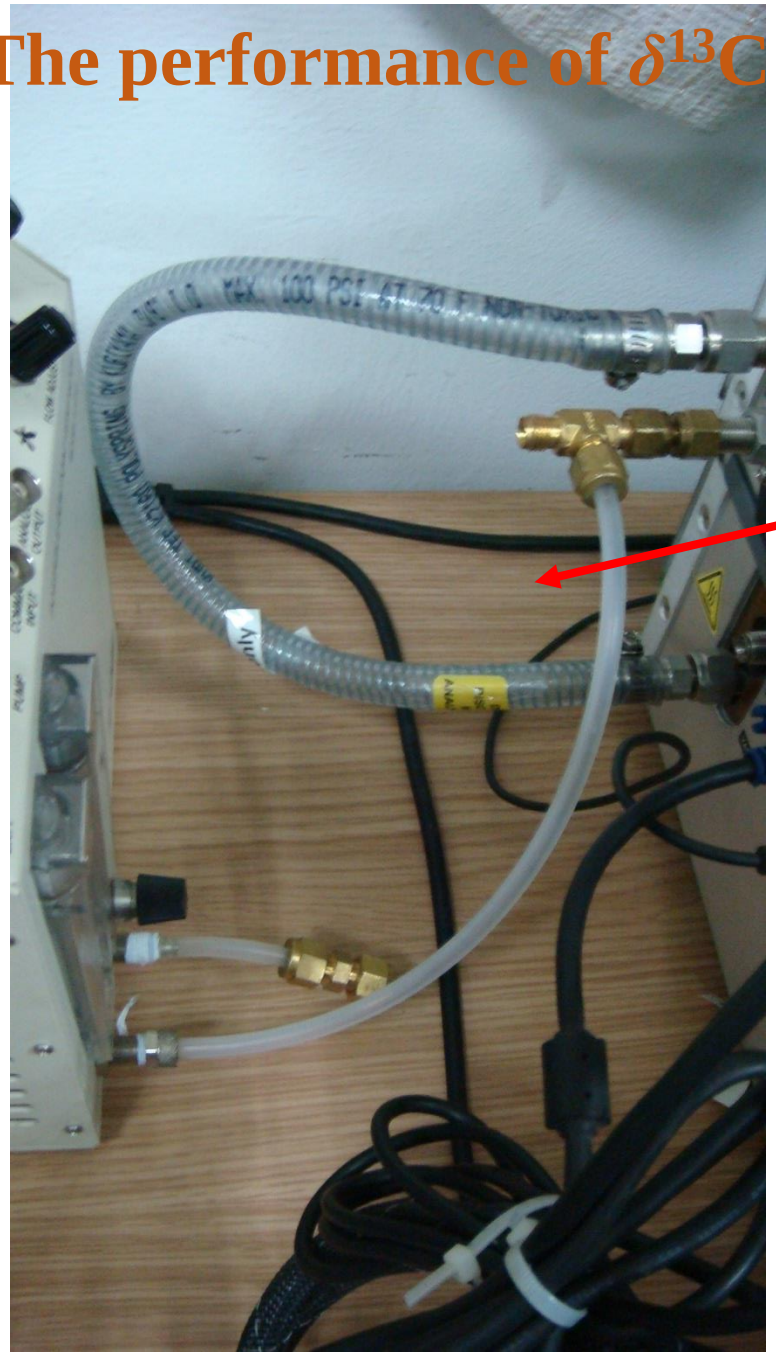

- Connect the CO_2 standard gas (second level standard gas, 439ppm) to the INLET of the dew point generator.
- Set the delivery pressure of the CO_2 gas to 1 psi.
- Connect one outlet of the dew point generator to the inlet of the Picarro analyzer with a union T. One end of the union T is open to the room.
- The tubing between the DP and the Picarro analyzer is as short as possible.
- The second outlet of the dew point generator is completely blocked.
- Set the dew point outlet flow rate to 150 cc /min.
- Run the Picarro analyzer continuously without interruption.

4. Preliminary results

4.1 Correction of $\delta^{13}C$ for humidity interferences

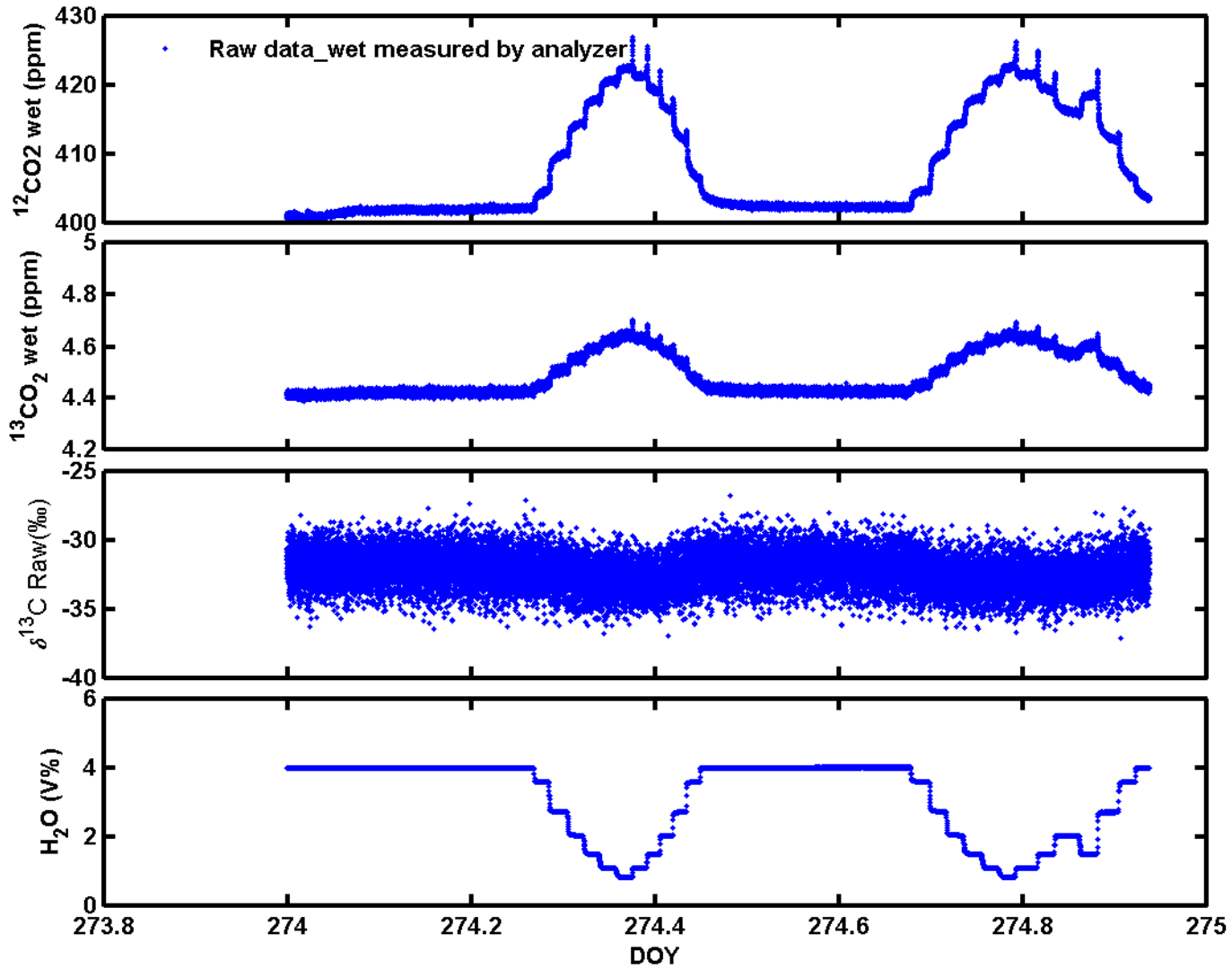

Fig.3 The time series of wet $^{12}CO_2$, wet $^{13}CO_2$, raw $\delta^{13}C$ and H_2O.

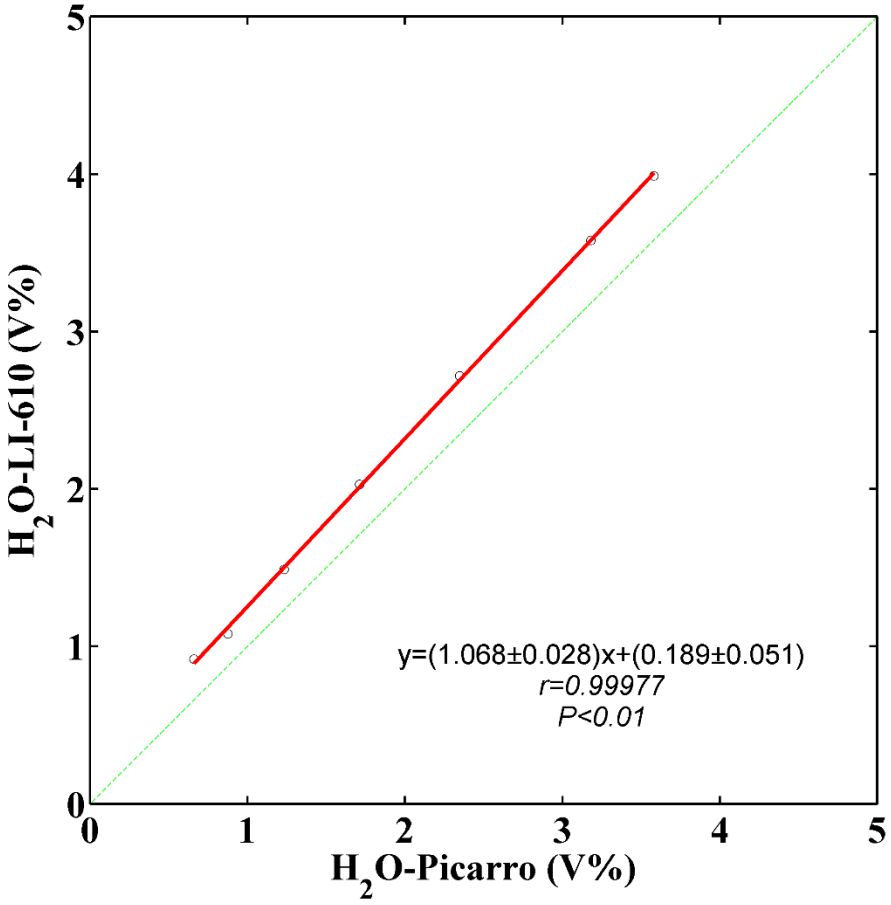

Fig.4 1VS1 H_2O mixing ratios.

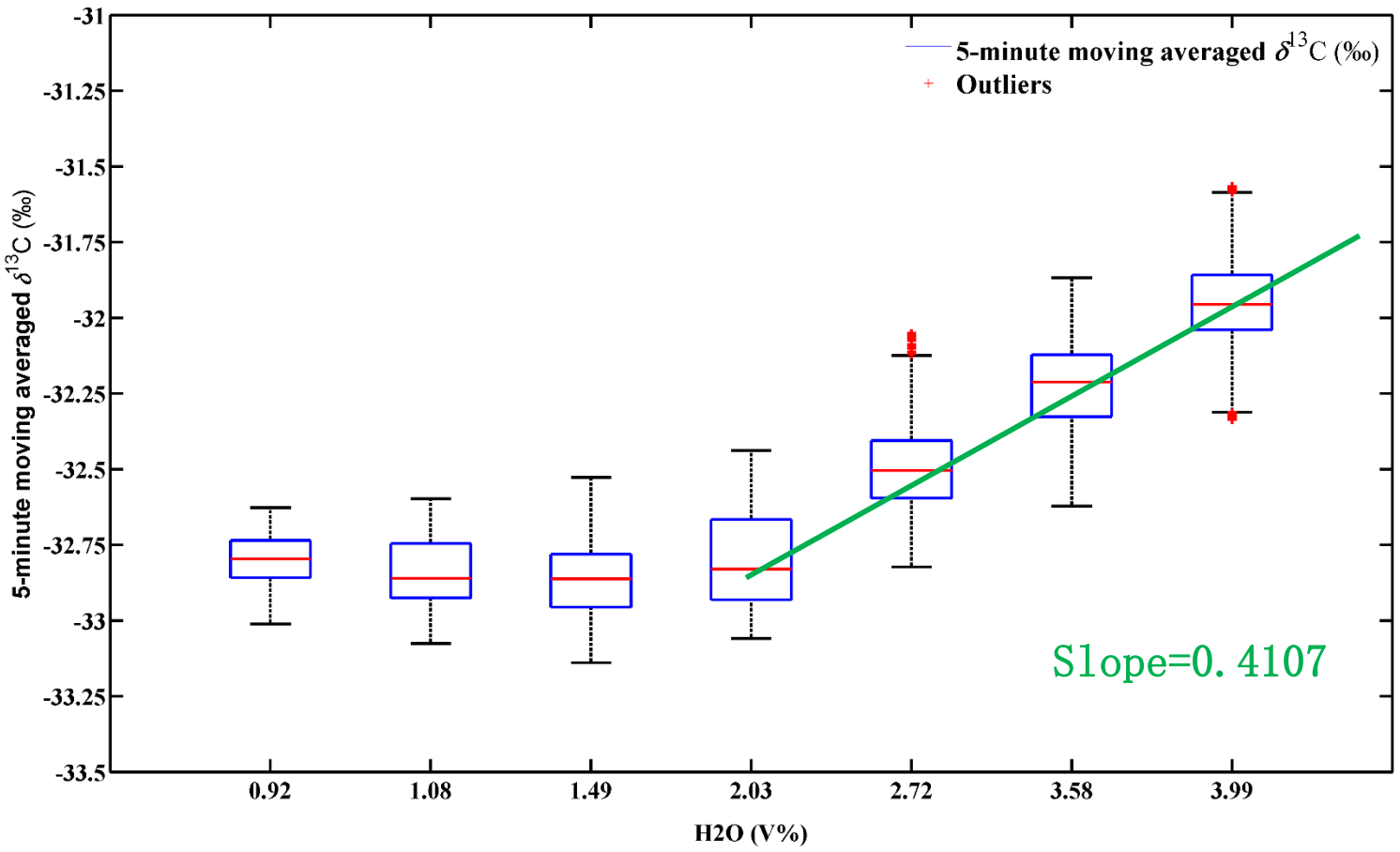

Fig.5 5-min moving averaged $\delta^{13}C$ under different H_2O mixing ratios.

4.2 Temporal variation of CO_2 and its stable isotope ratio

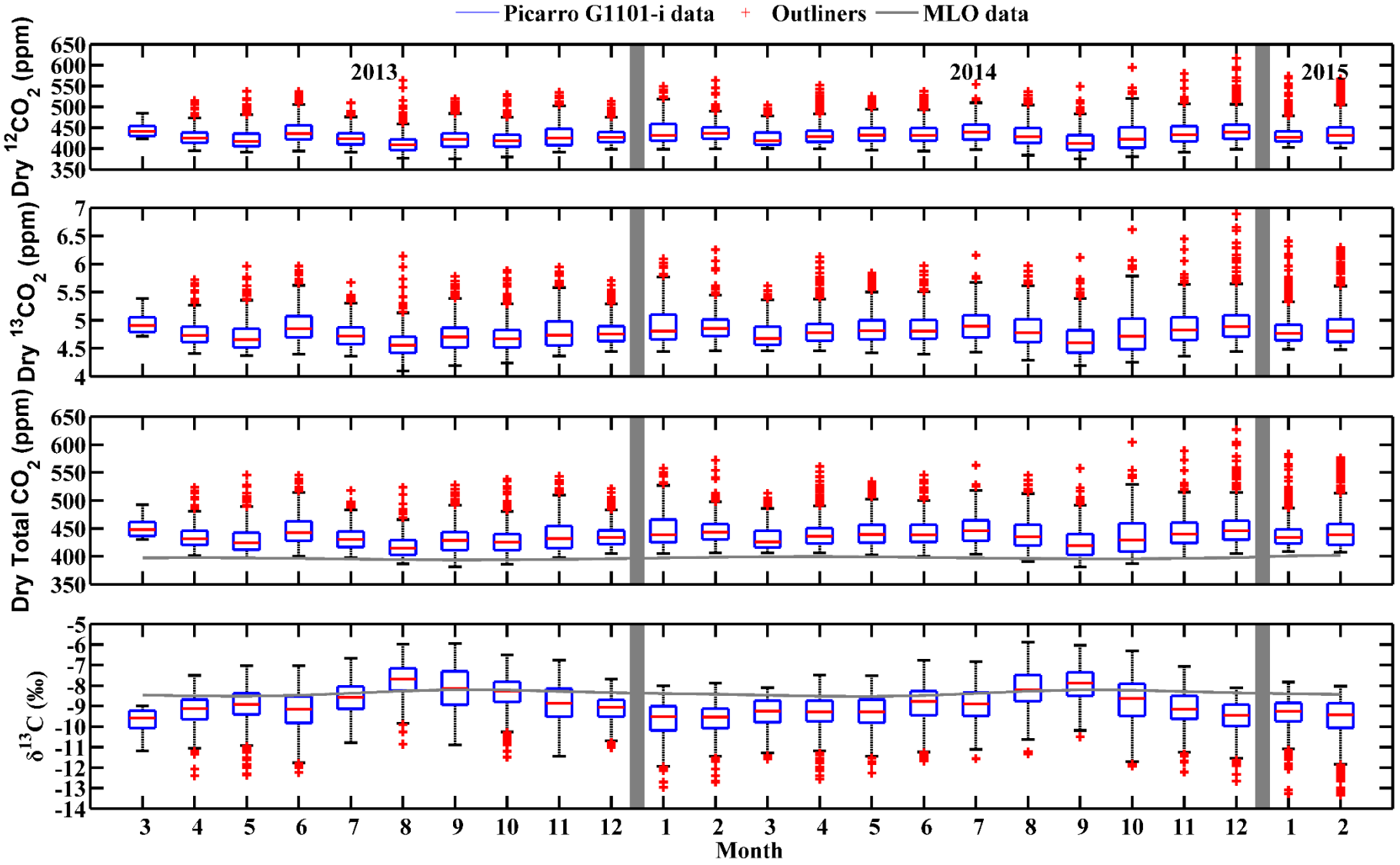

Fig.6 Monthly dry $^{12}CO_2$, dry $^{13}CO_2$, dry CO_2 and $\delta^{13}C$.

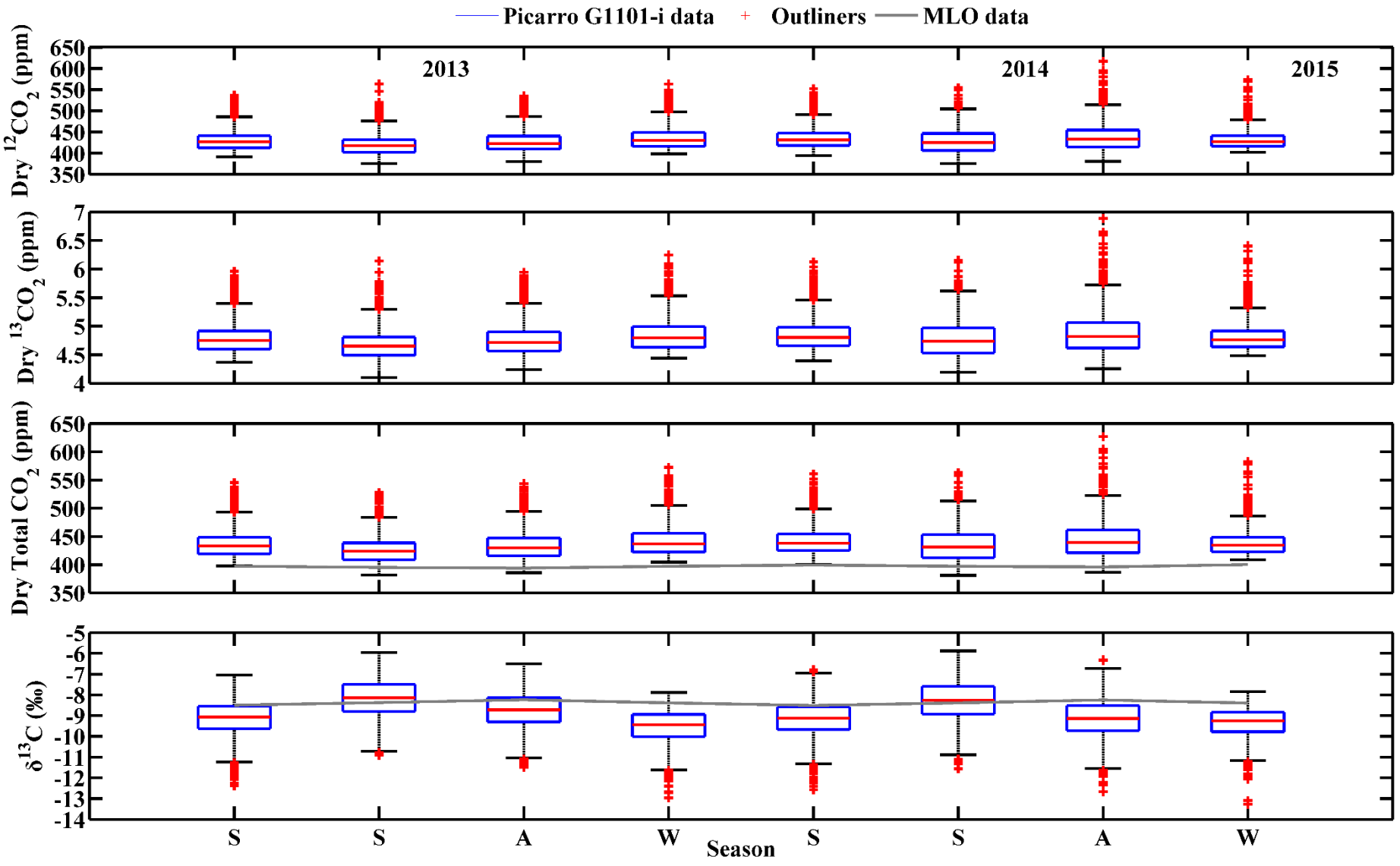

Fig.7 Seasonal dry $^{12}CO_2$, dry $^{13}CO_2$, dry CO_2 and $\delta^{13}C$.

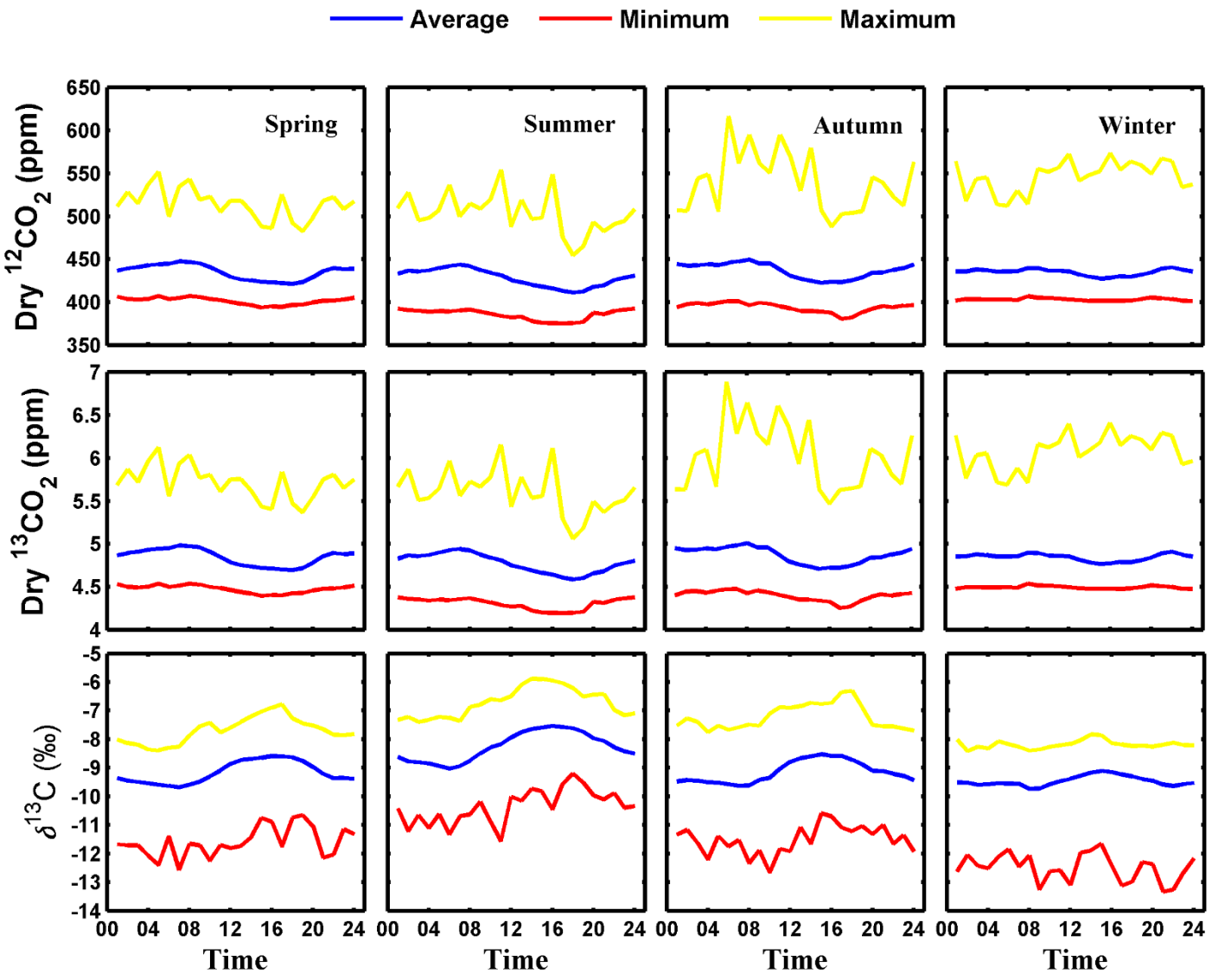

Fig.8 Diurnal variation of dry $^{12}CO_2$, dry $^{13}CO_2$ and $\delta^{13}C$ during four seasons.

4.3 $\delta^{13}C_S$ calculated using Miller's method

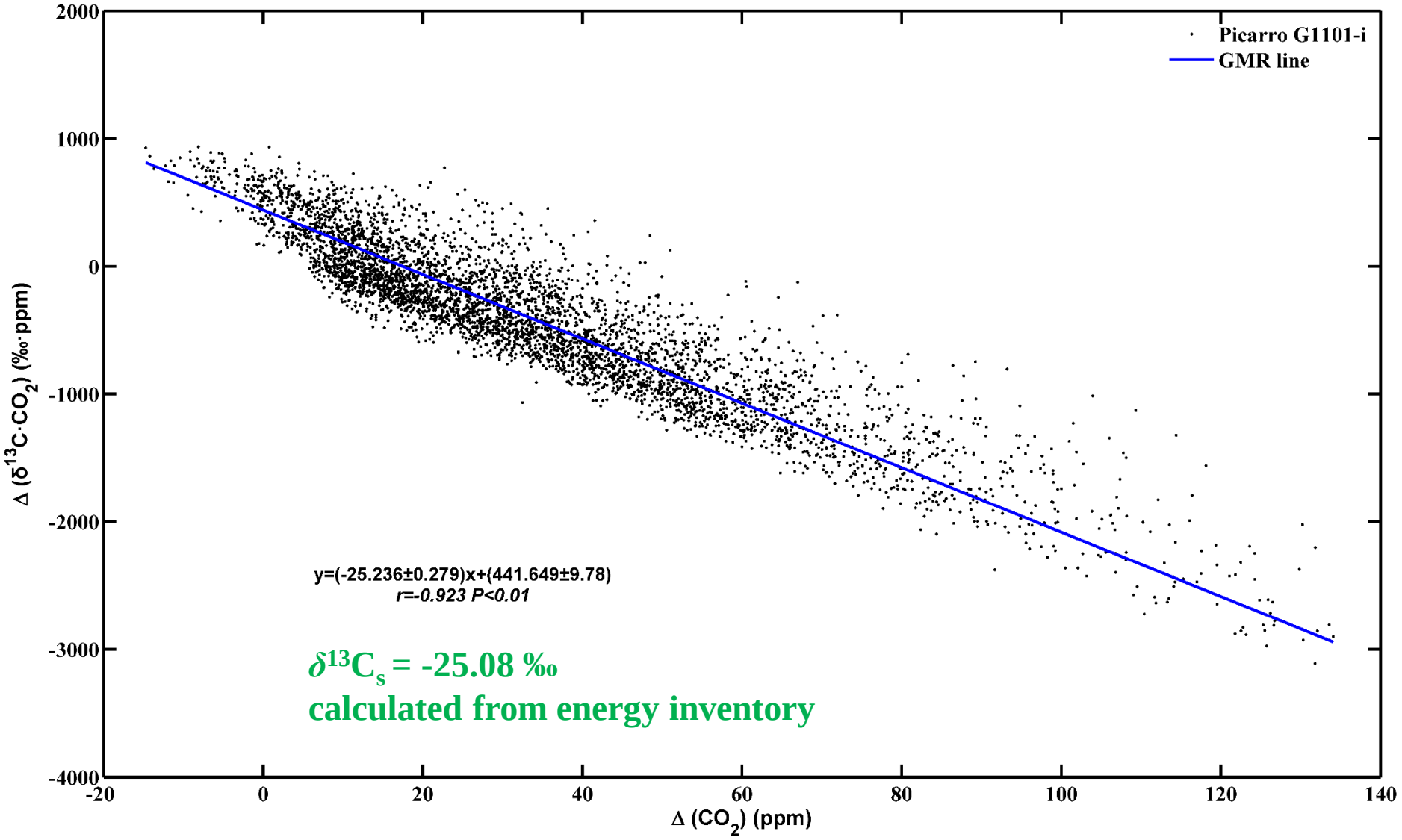

Fig.9 $\delta^{13}C_s$ of Nanjing (Mar, 2013 to Feb, 2015).

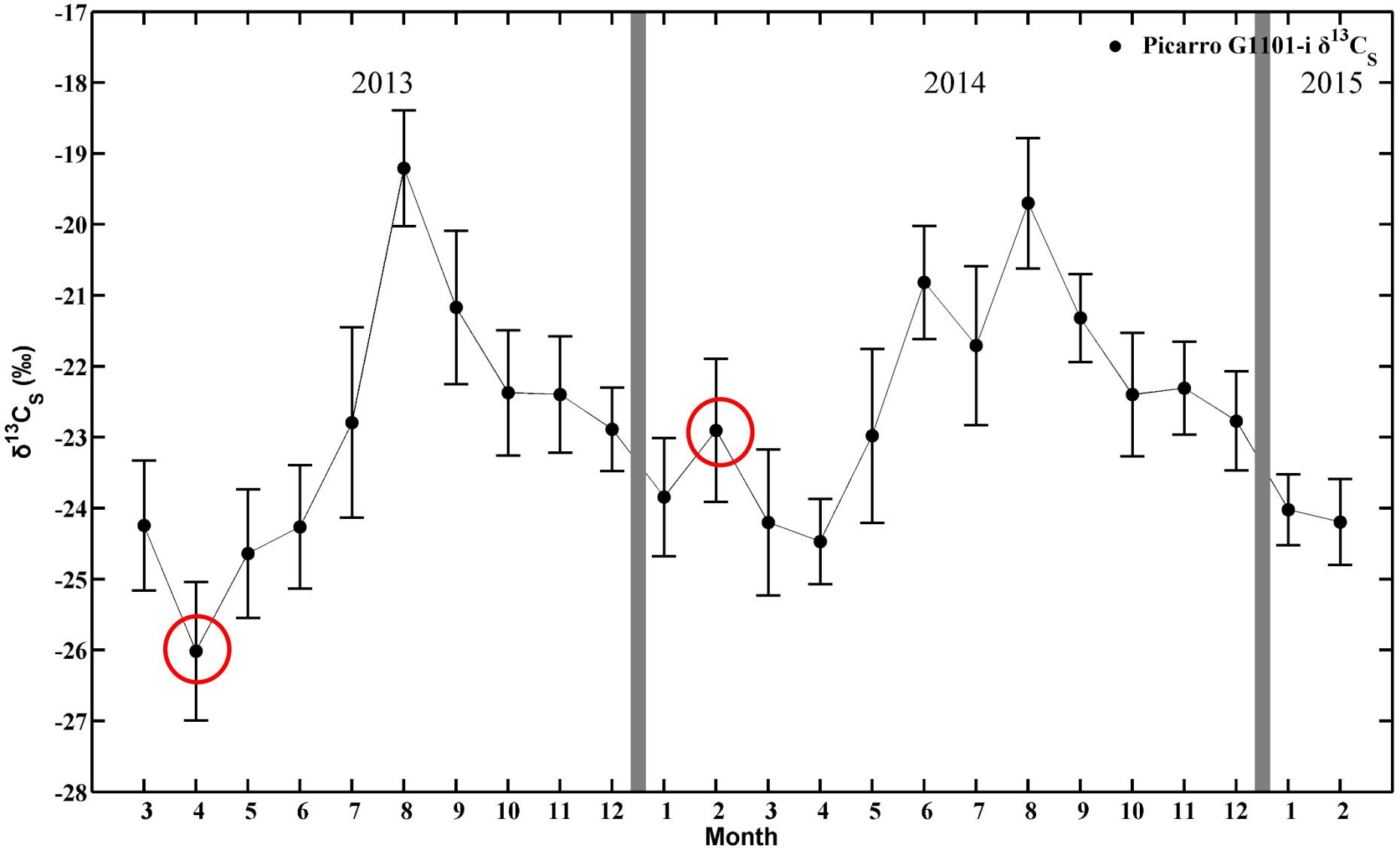

Fig.10 Temporal variation of $\delta^{13}C_s$ in Nanjing (Mar, 2013 to Feb, 2015).

4.4 Partition of monthly anthropogenic and biogenic CO_2 sources

Table 4 Main CO_2 sources

Sources	$\delta^{13}C$ (‰)	Reference
Fossil	-25.08	this study
Cement	0	Andres, 1998
Plant	-26.2	Pataki, 2003a

Table 5 Main fossil fuel

Sources	Percentage	$\delta^{13}C$ (‰)
Coal	64.10	-23.97
Coke	8.27	-23.97
Crude oil	1.33	-26.6
Gasoline	3.97	-25.45
Kerosene	0.89	-25.5
Diesel	4.757	-25.23
Fuel oil	1.84	-37.0921
Natural gas	2.83	-37.7
Total	100	-25.08

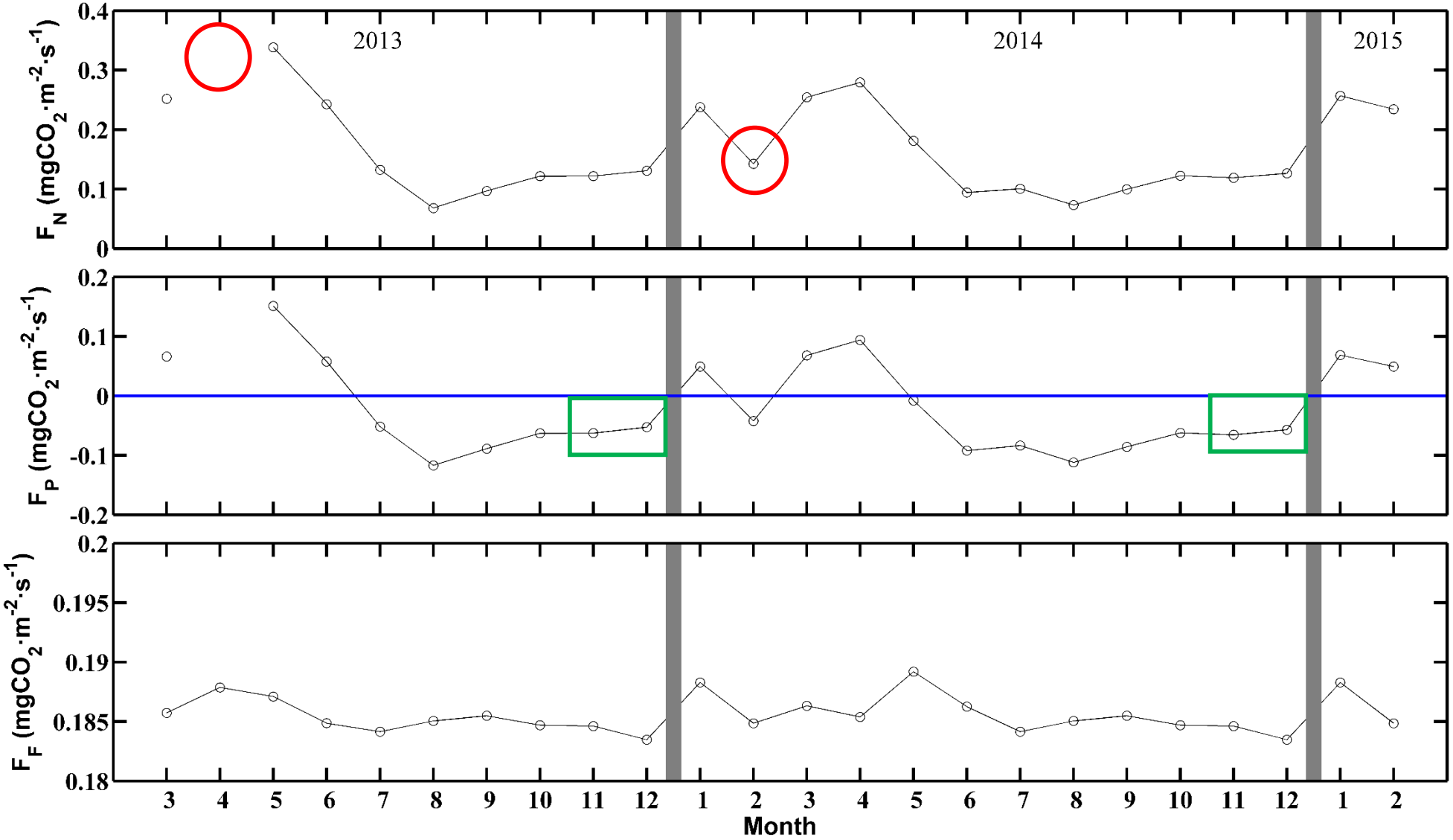

Fig.11 The monthly F_F, F_P and F_N estimited from mass balance equations.

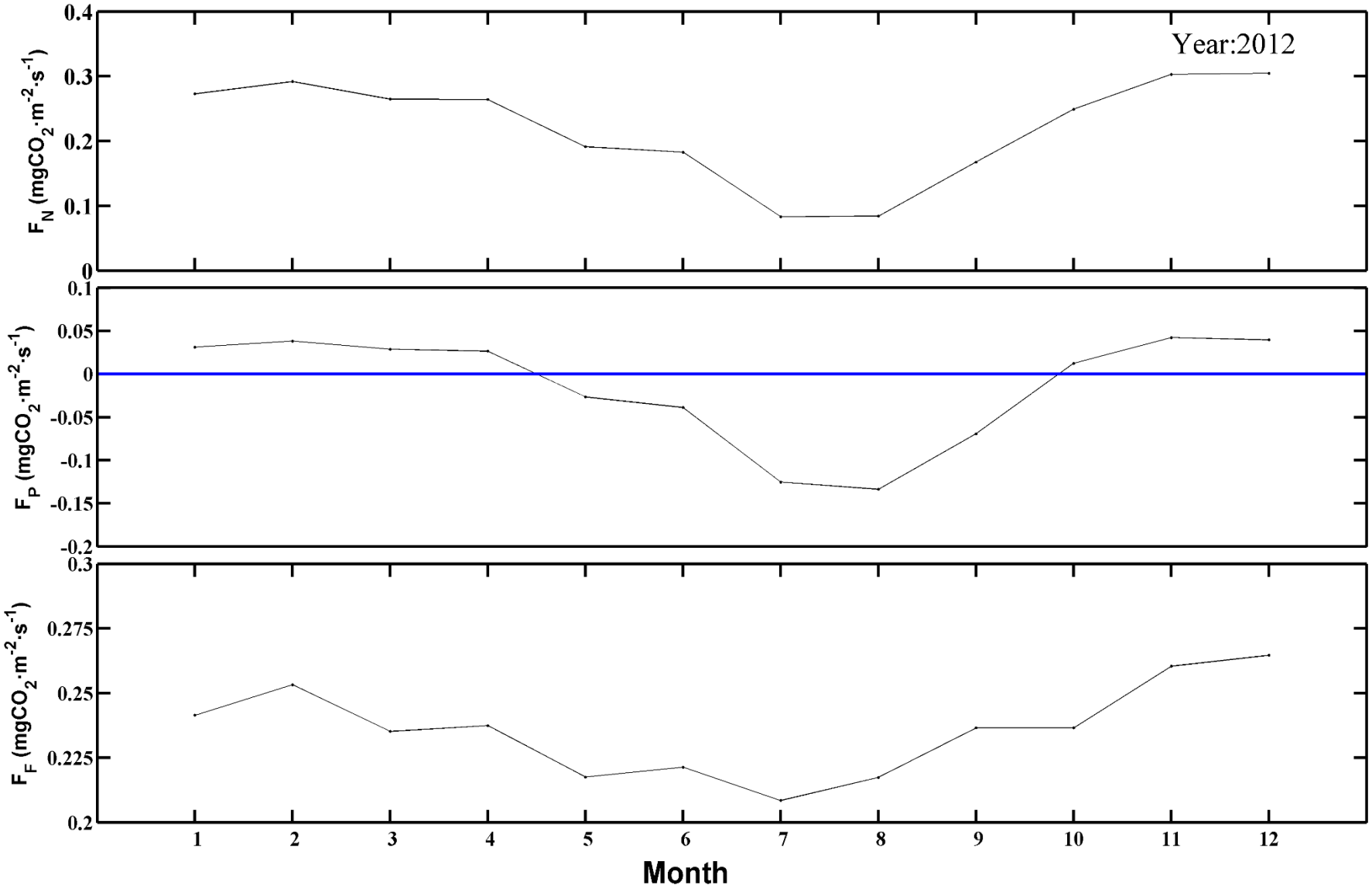

Fig.12 The monthly F_F, F_P and F_N based on remote sensing (Carbon Tracker) in 2012.

Table 6. Comparison between CO_2 flux calculated by Picarro and Carbon Tracker.

$mgCO_2/(m^2\ s)$	Time	F_N	F_P	F_F	Analyzer
Nanjing	Mar, 2013 ~ Feb, 2015	0.166	-0.019	0.186	Picarro
Nanjing	2012	0.222	-0.014	0.237	CT
Nanjing	Summer, 2014	0.517			Licor-840
Nanjing	2009	0.32			Picarro
Chicago	1992	0.44-1.672			

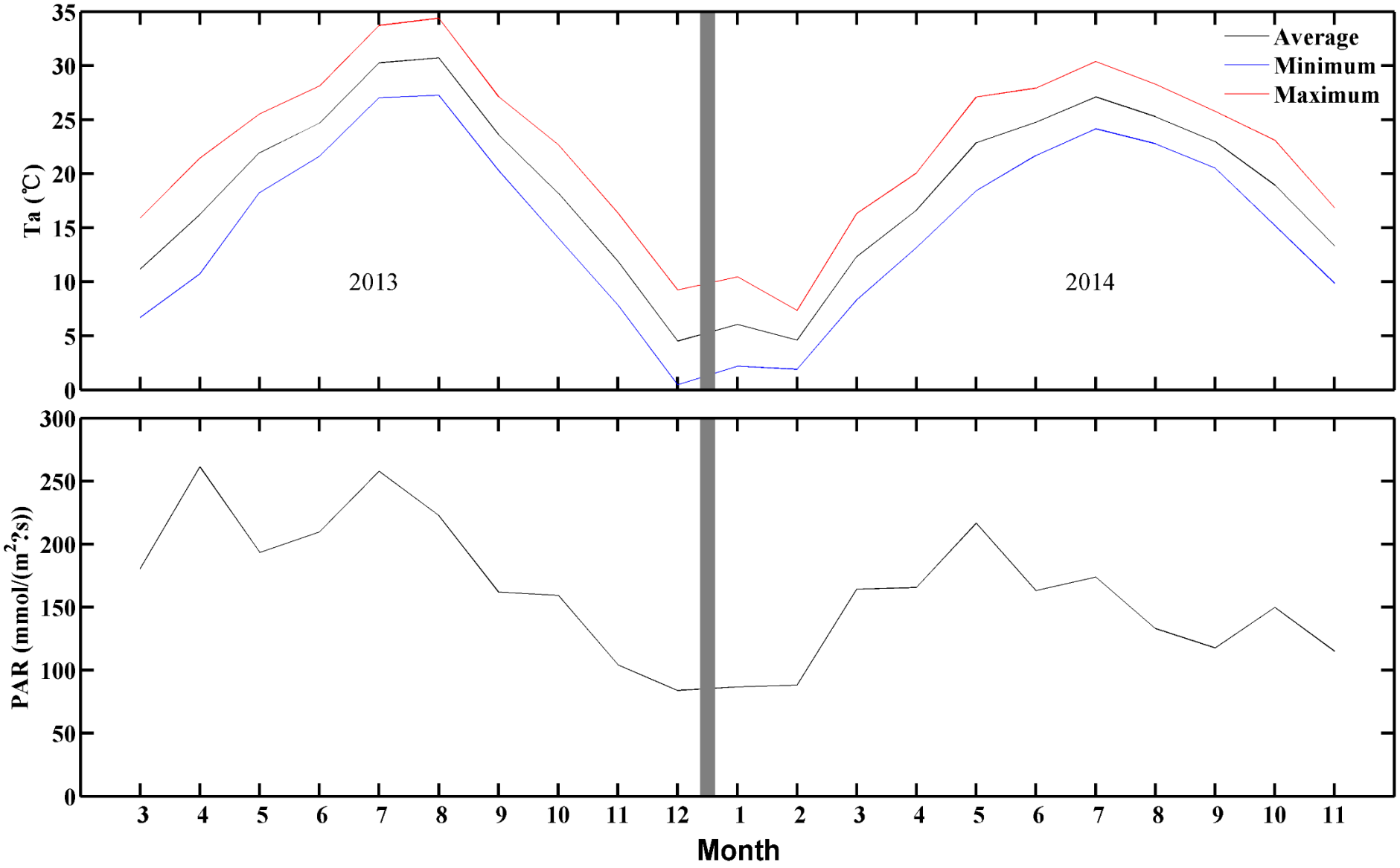

Fig.13 The time series of Ta and PAR.

4.5 Components of the nighttime CO_2 mixing ratio

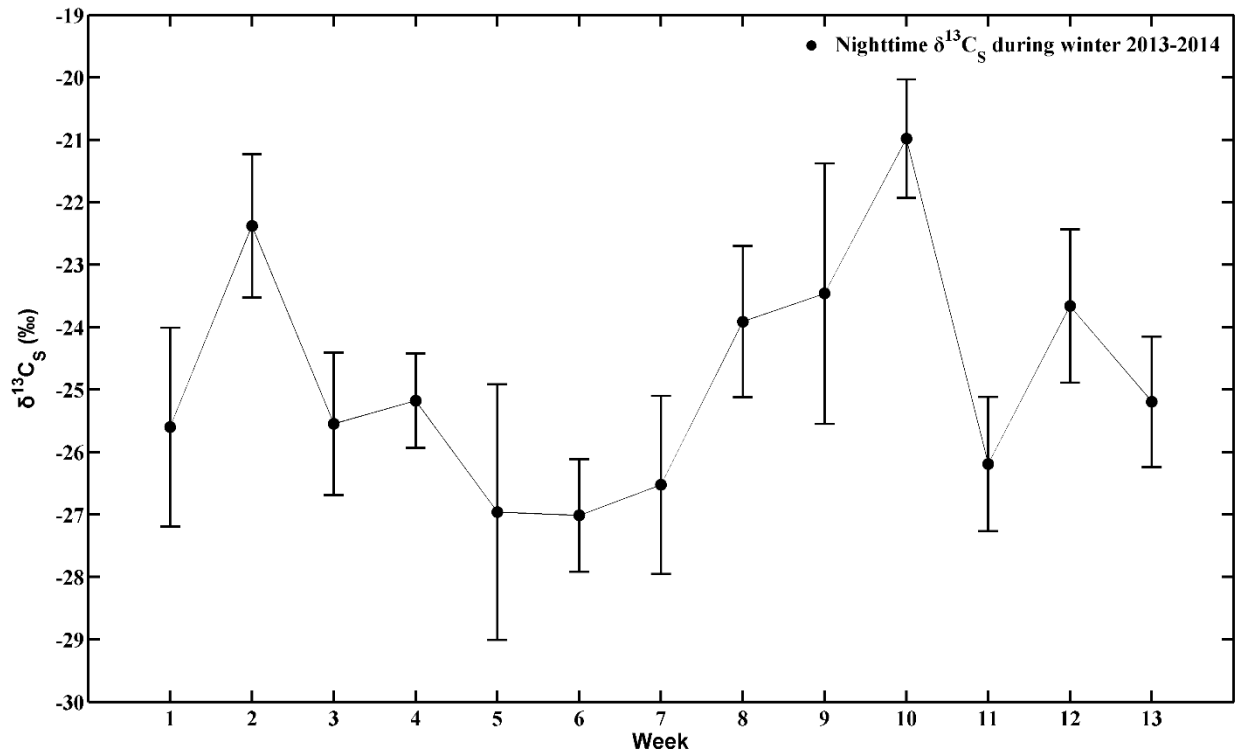

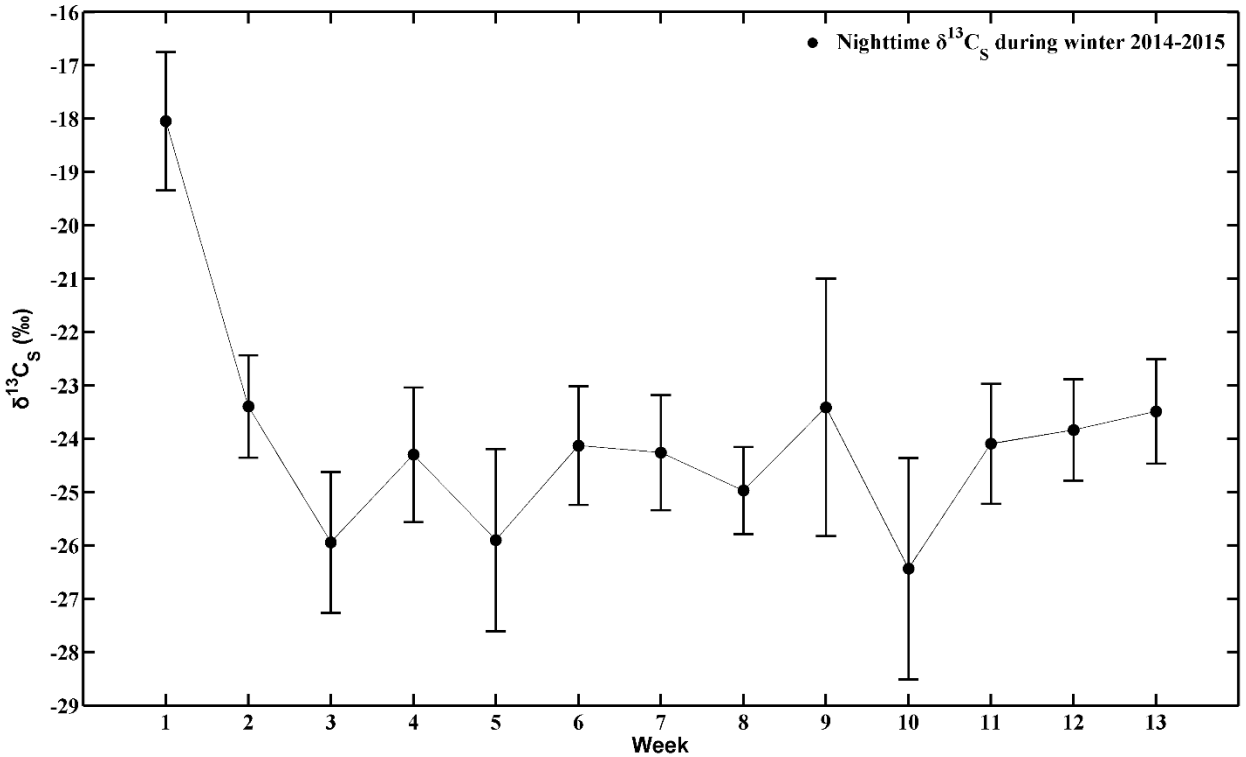

Fig.14 Weekly $\delta^{13}C_s$ during winter in 2013-2014 and 2014-2015.

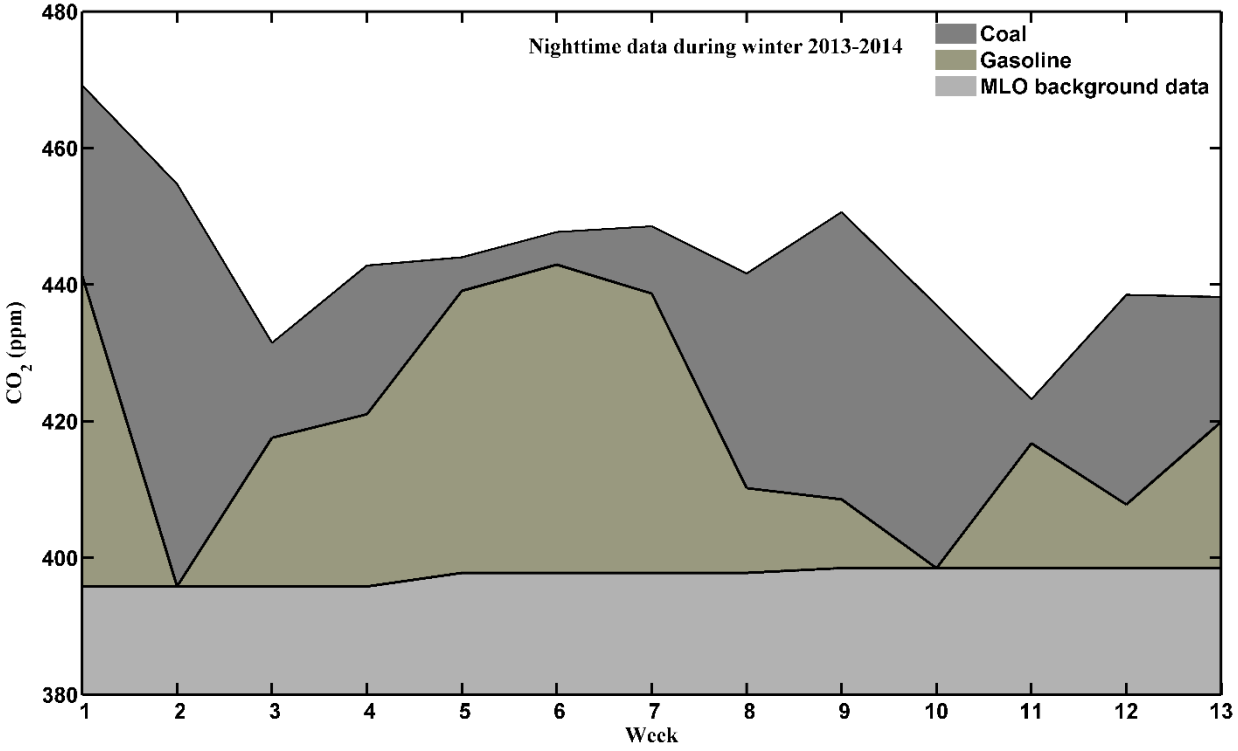

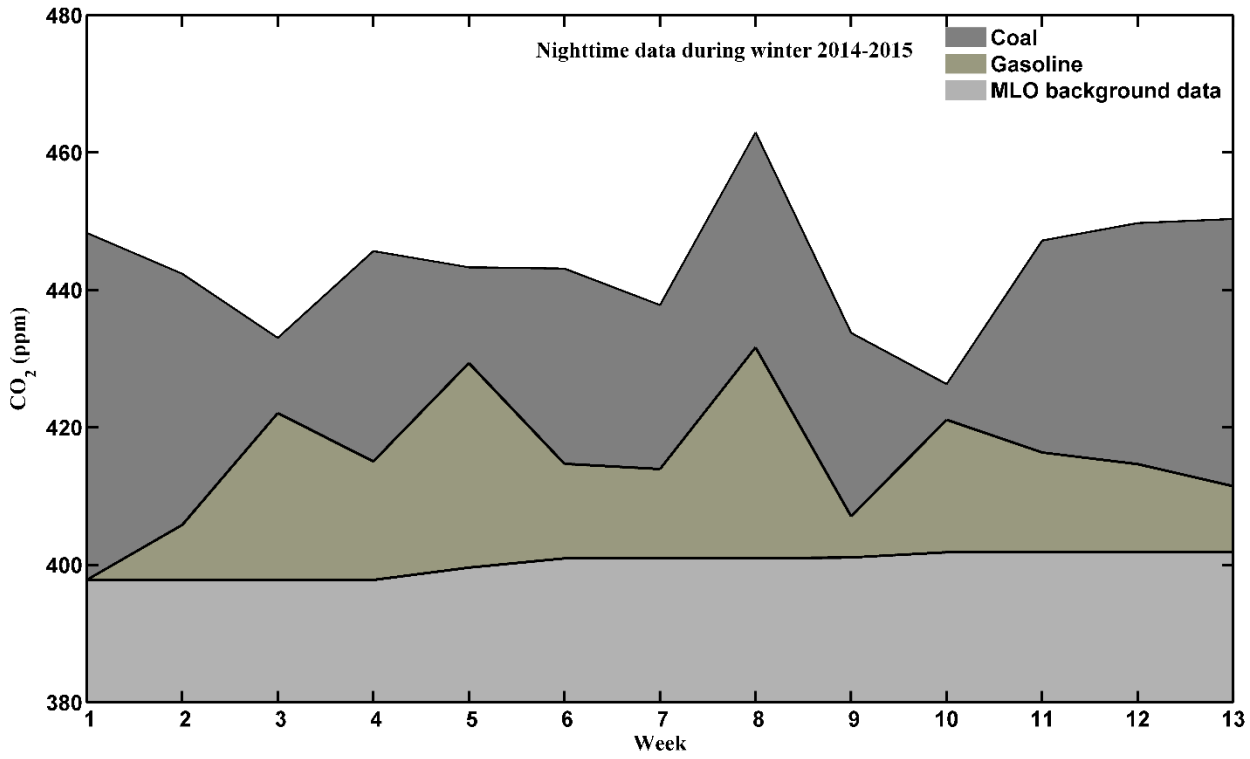

Fig.15 Weekly components of the nighttime CO_2 mixing ratio during winter in 2013-2014 and 2014-2015.

4.6 The relationship between CO_2 emission and other air pollutants

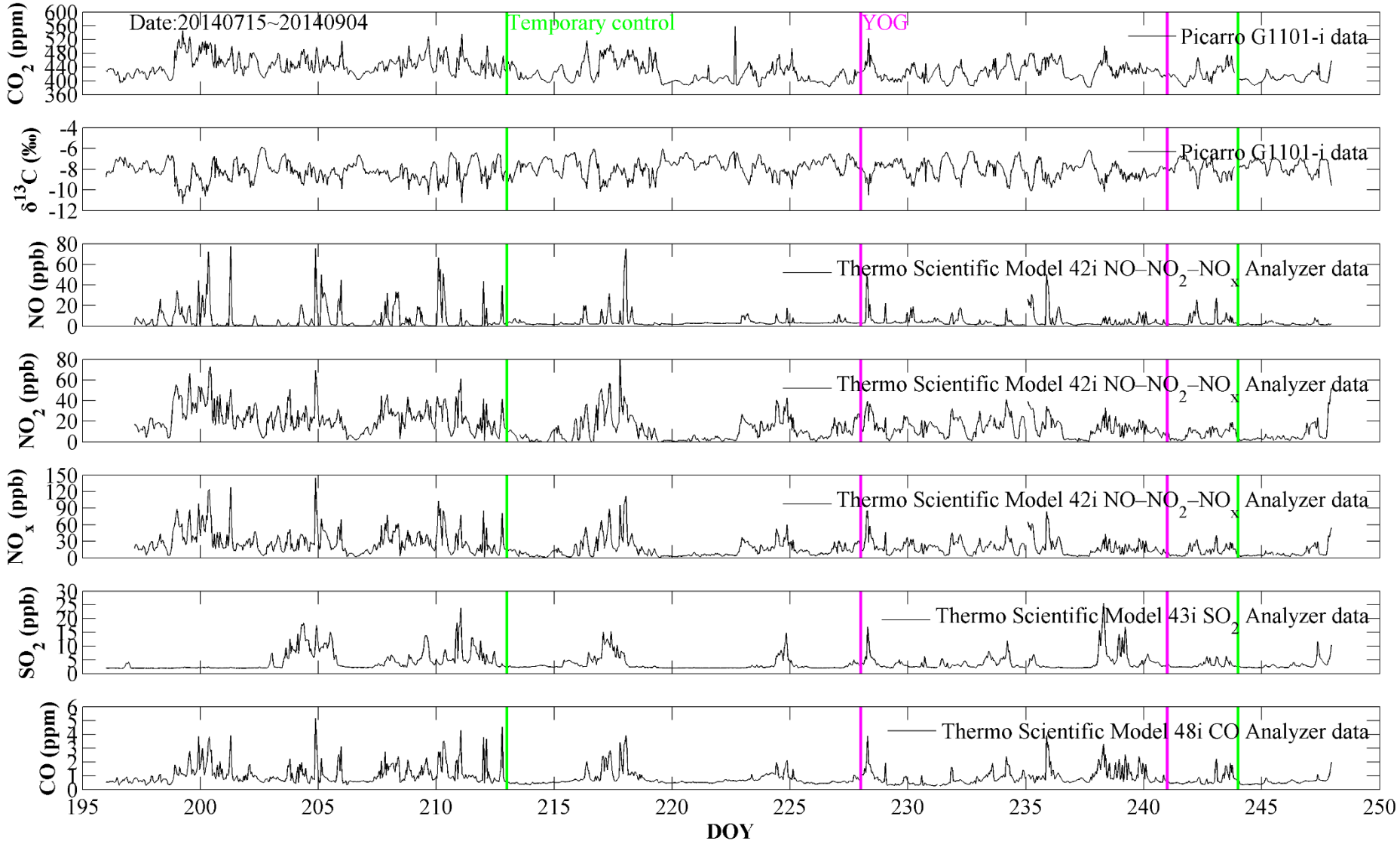

Fig.16 The time series of CO_2,
$\delta^{13}C$, NO, NO_2, NOx, SO_2 and CO concentration during YOG.

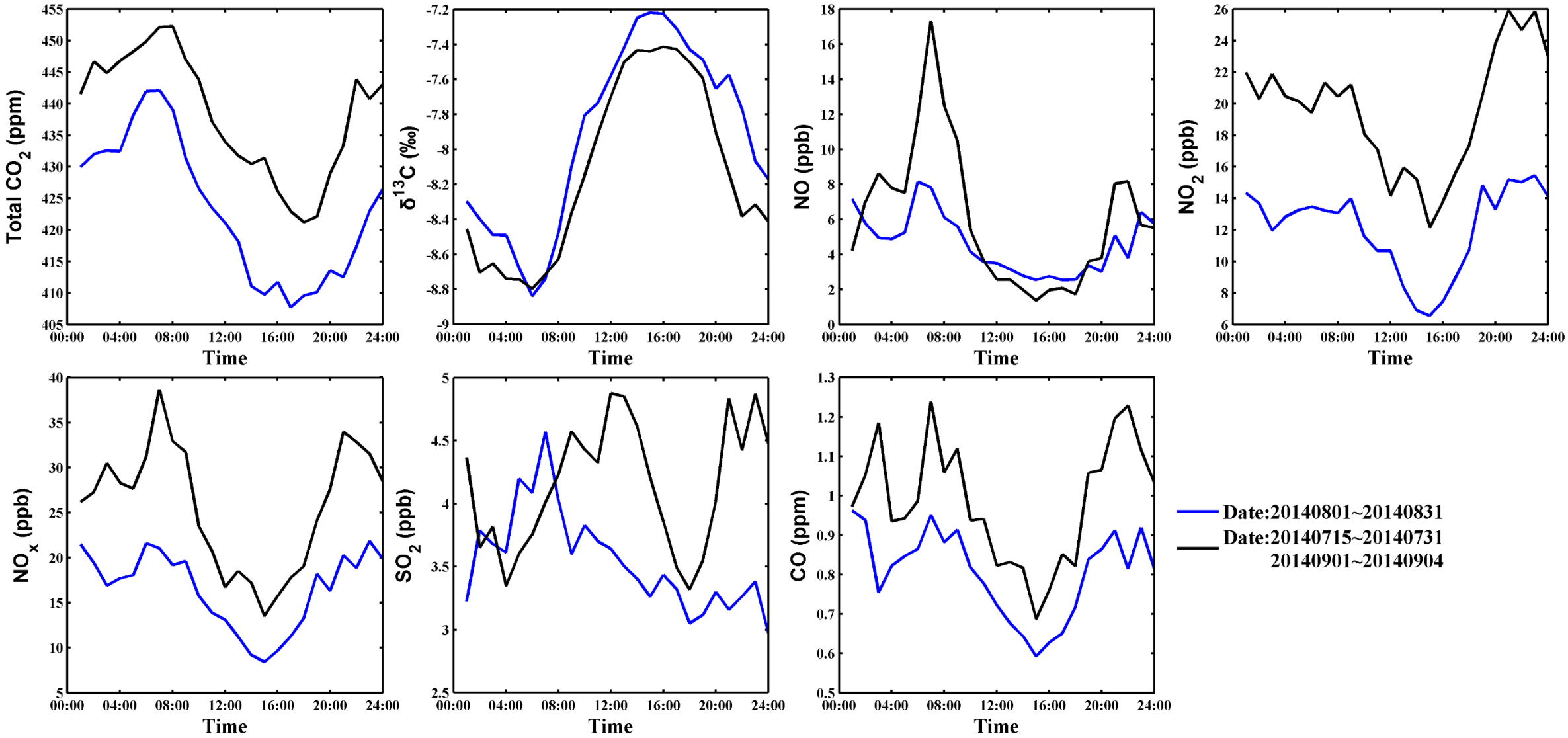

Fig.17 The diurnal composition of CO_2, $\delta^{13}C$, NO, NO_2, NOx, SO_2 and CO concentration during YOG.

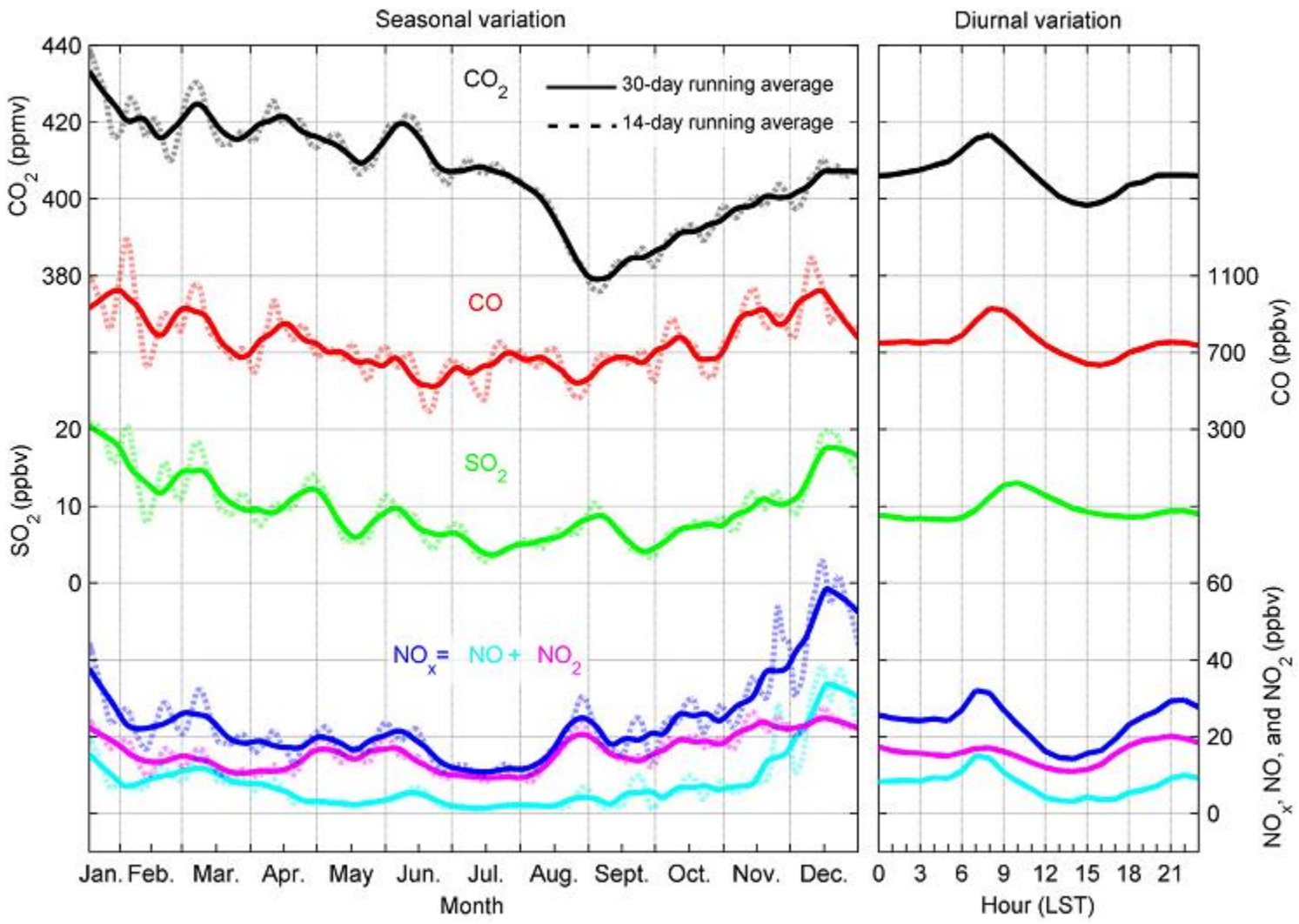

Fig.18 The monthly time series and diurnal composition of CO_2, $\delta^{13}C$, NO, NO_2, NOx, SO_2 and CO concentration in Gulou site in 2011.

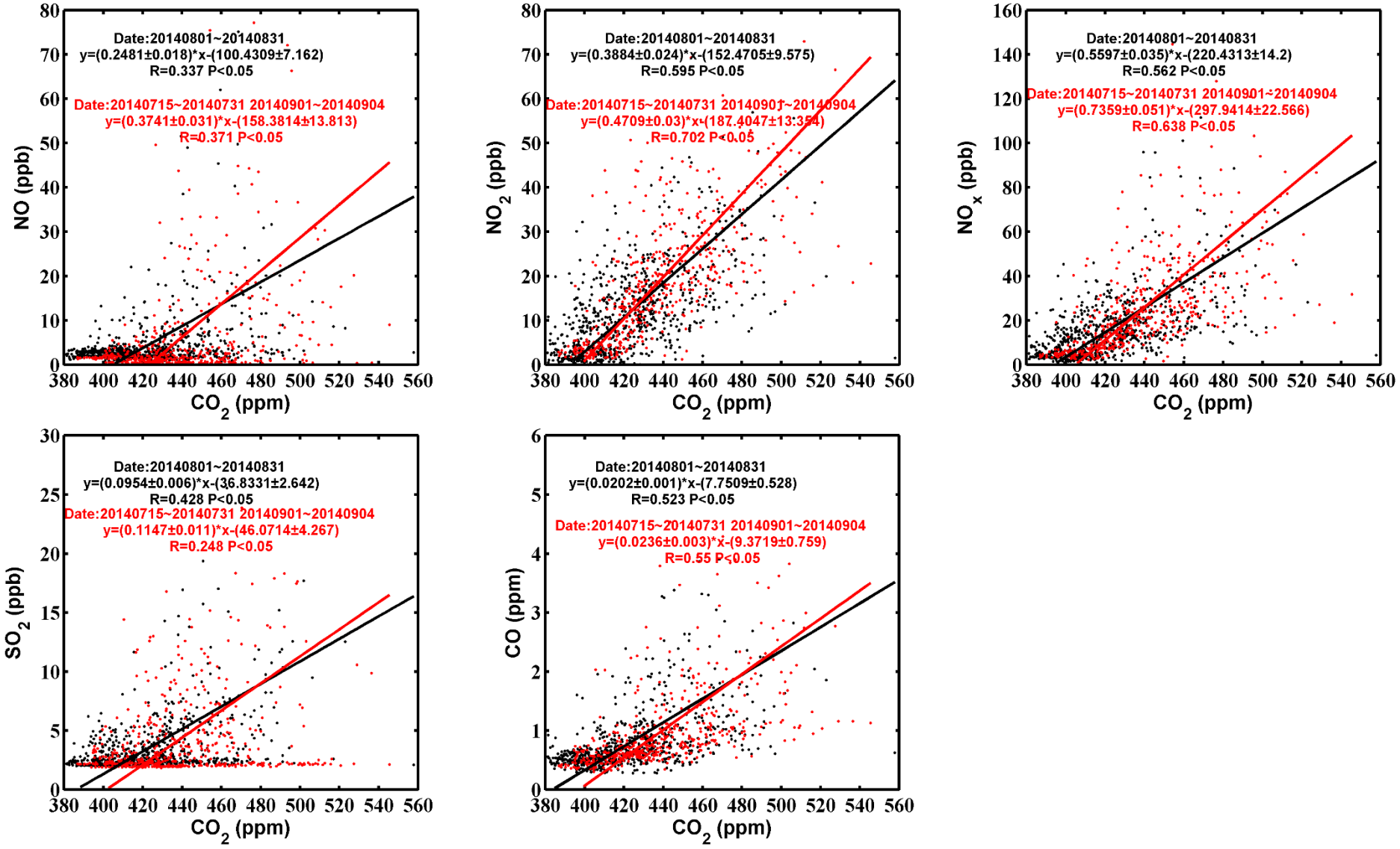

Fig.19 The relationship between CO_2 and $\delta^{13}C$, NO, NO_2, NOx, SO_2 and CO, respectively.

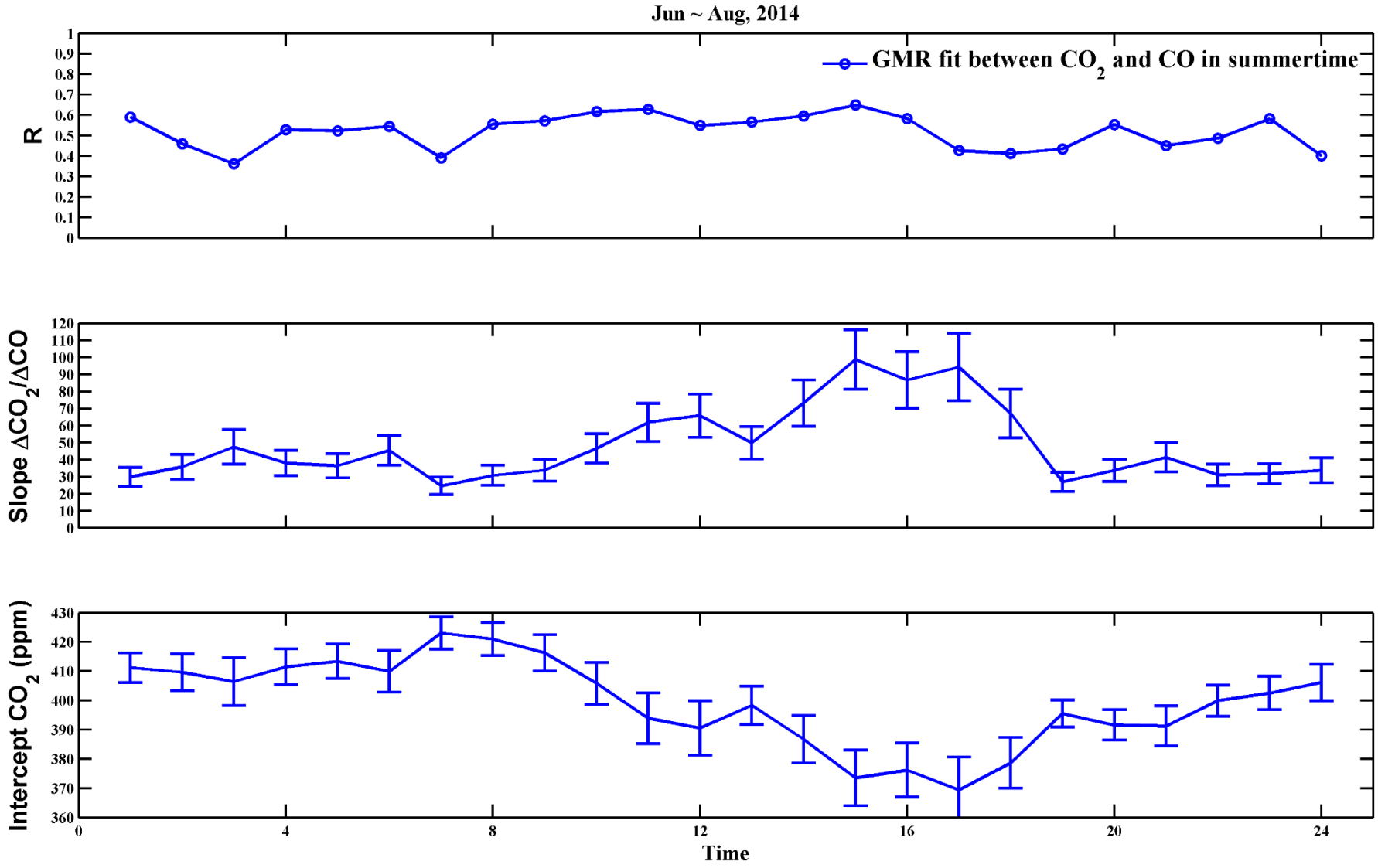

Fig.20 The relationship between CO and CO_2.

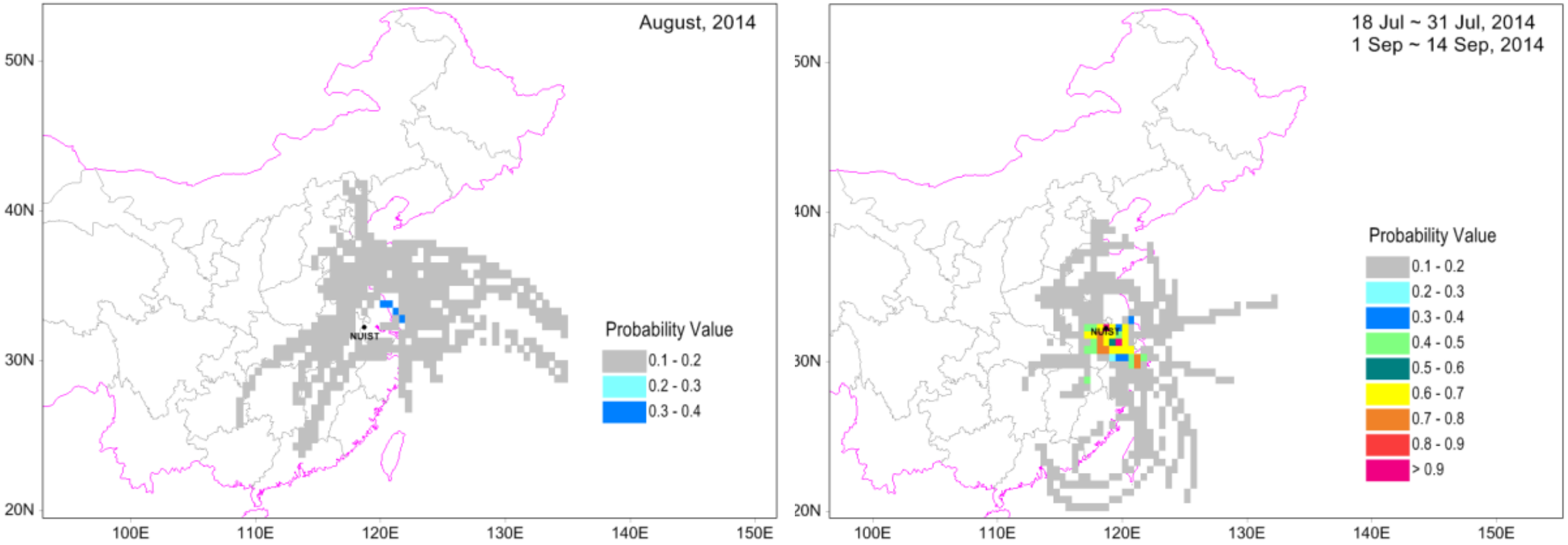

Fig.21 The WPSCF
during temporory contorls (left) and without temporory contorls (right).

4.7 The Potential dependence of $\delta^{13}C$ on CO_2 concentration

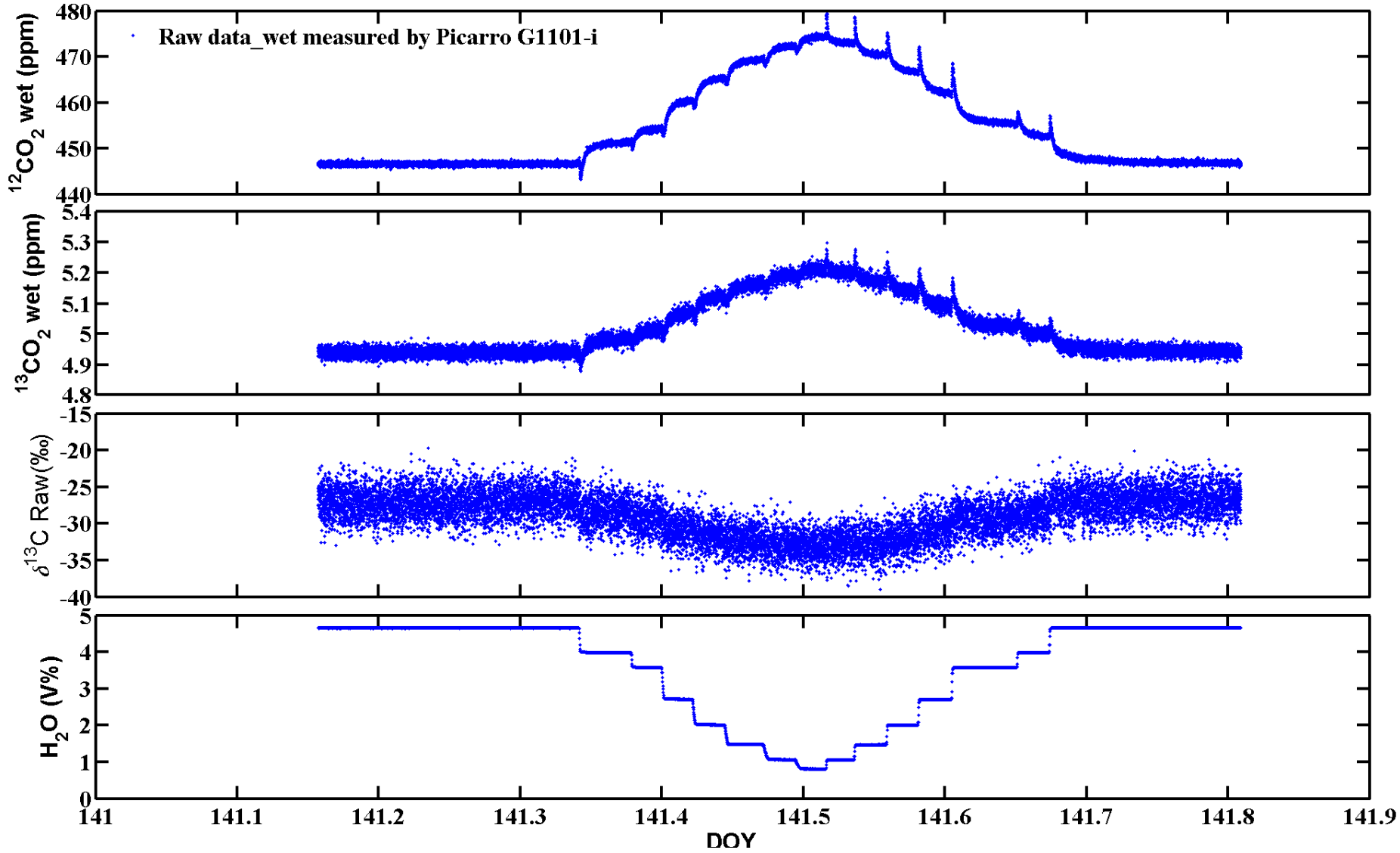

Fig.22 The time series of wet $^{12}CO_2$, wet $^{13}CO_2$, raw $\delta^{13}C$ and H_2O with 488ppm CO_2 gas.

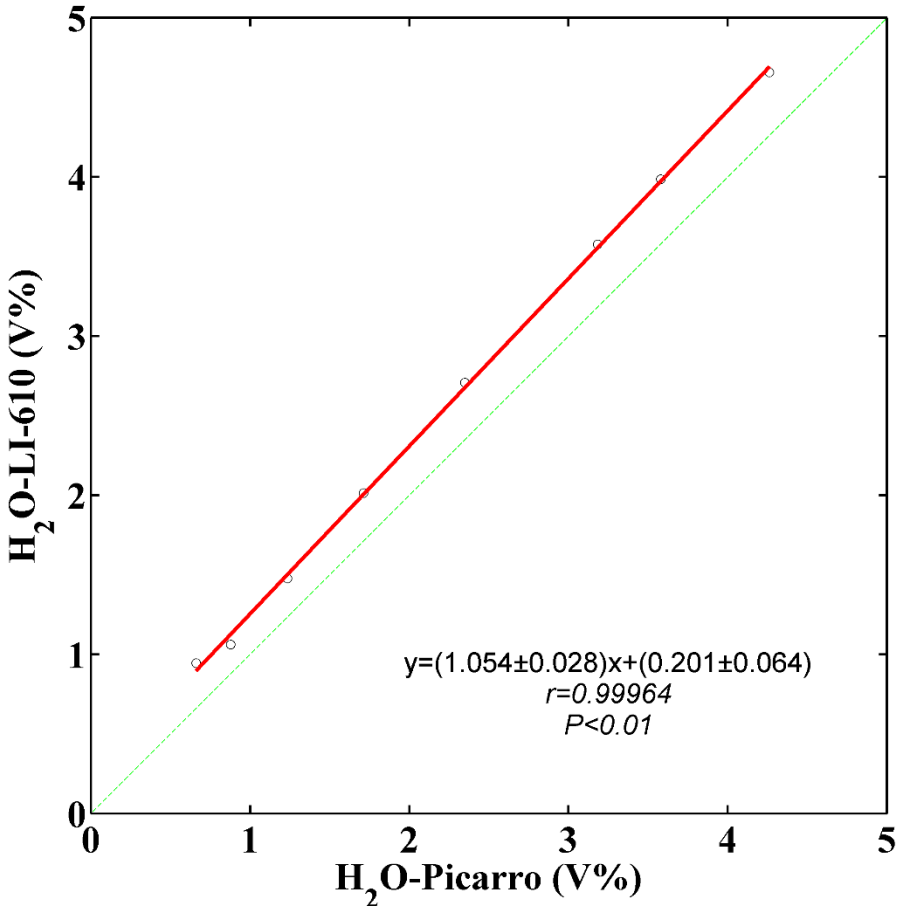

Fig.23 1VS1 H_2O mixing ratios with 488ppm CO_2 gas.

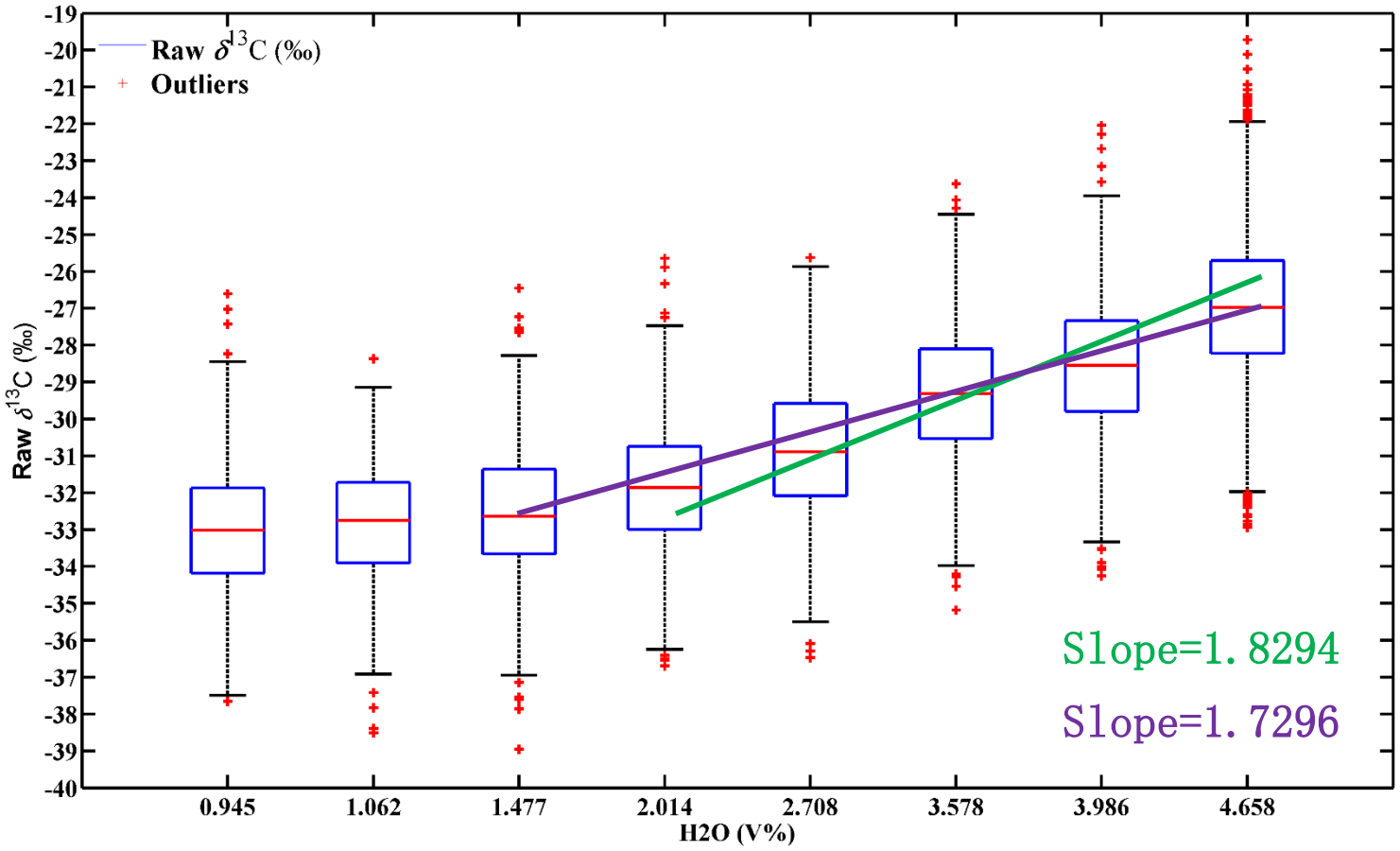

Fig.24 Raw $\delta^{13}C$ under different H_2O mixing ratios with 488ppm CO_2 gas.

5. Conclusion

- 1. Every 1V% increase in humidity can lead to less negative 0.4107 ‰ when H_2O mixing ratio is higher than 2.014V%. The seasonal variation of $\delta^{13}C_s$ ranges between -7.55 ‰ and -9.71‰, while CO_2 concentration changes from 403.41ppm to 465.77ppm.

- 2. $\delta^{13}C_s$ is -25.24‰ during these 2-year observation, ranging from -26.02‰ to -19.21‰. Nanjing is the CO_2 source in whole year. Monthly $\delta^{13}C_s$ can be used as a tool to partition the anthropogenic and biogenic CO_2 sources. The annual net CO_2 flux, plant CO_2 flux and fossil fuel CO_2 flux can reach 0.166mgCO_2/(m^2 s),-0.019mgCO_2/(m^2 s) and 0.186mgCO_2/(m^2 s) respectively, which are similar with the results of Carbon Tracker. The weekly $\delta^{13}C_s$ also can be adopted to divide main anthropogenic CO_2 sources into coal and gasoline, although parts of the calculation still failed to achieve this evaluation.

5. Conclusion

- 3. CO and NO_2 are promising tools to further partition potential anthropogenic CO_2 emission. NO_2 concentration might be evaluated according the relationship between NO_2 and CO_2.

- 4. Regional and temporary control on CO_2 emission can influence CO_2 concentration and its stable isotope in a short time scale.

- 5. $\delta^{13}C_s$ might also suffer from the dependence of CO_2 concentration.

6 Next Work

- 1. Sensitivity tests
- 2. Concentration dependence

Thank You!